Discovery of a Novel Series of Potent and Selective Alkynylthiazole-Derived PI3Kγ Inhibitors

Upul K. Bandarage,* Alex M. Aronov, Jingrong Cao, Jon H. Come, Kevin M. Cottrell, Robert J. Davies, Simon Giroux, Marc Jacobs, Sudipta Mahajan, David Messersmith, Cameron S. Moody, Rebecca Swett, and Jinwang Xu

ACCESS | Metrics & More | Article Recommendations | Supporting Information

1 PI3Kγ K_i = 0.002 μM
MDR1 ER = 18

32 PI3Kγ K_i = 0.003 μM
MDR1 ER = 0.9
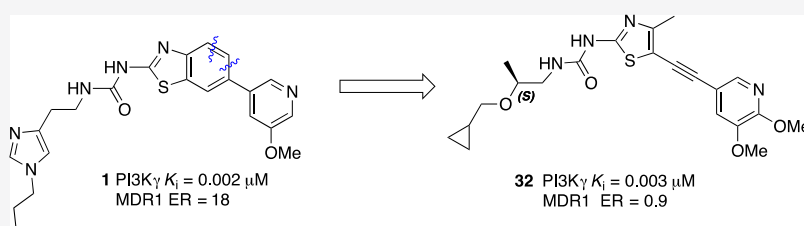
ABSTRACT: Phosphoinositide 3-kinases (PI3Ks) are a family of enzymes that control a wide variety of cellular functions such as cell growth, proliferation, differentiation, motility, survival, and intracellular trafficking. PI3Kγ plays a critical role in mediating leukocyte chemotaxis as well as mast cell degranulation, making it a potentially interesting target for autoimmune and inflammatory diseases. We previously disclosed a novel series of PI3Kγ inhibitors derived from a benzothiazole core. The truncation of the benzothiazole core led to the discovery of a structurally diverse alkynyl thiazole series which displayed high PI3Kγ potency and subtype selectivity. Further medicinal chemistry optimization of the alkynyl thiazole series led to identification of compounds such as **14** and **32**, highly potent, subtype selective, and CNS penetrant PI3Kγ inhibitors. Compound **14** showed robust inhibition of PI3Kγ mediated neutrophil migration *in vivo*.

KEYWORDS: *PI3Kγ, benzothiazole, alkynylthiazole, neutrophil migration*

The phosphoinositide 3-kinases (PI3Ks) are lipid kinases that phosphorylate the 3-hydroxyl group of the inositol ring of phosphatidylinositol (PI) substrates within the plasma membrane and intracellular compartments.[1] PI3Ks control a wide variety of cellular signaling pathways, including migration, proliferation, differentiation, and vesicular trafficking.[2] Based on sequence homology and lipid substrate specificity, PI3Ks are divided into three classes. The class I PI3Ks (PI3Kα, PI3Kβ, PI3Kγ, and PI3Kδ) are the most extensively studied and are further divided into two subclasses: 1A and 1B.[3] Class IA PI3Ks (α, β, δ) contain p110α, p110β, and p110δ as catalytic subunits and are activated by tyrosine kinase receptor signaling while class IB PI3Ks contain only p110γ as catalytic subunit and are activated by GPCRs via its βγ regulatory subunits.[3,4] PI3Kα and PI3Kβ are ubiquitously expressed and play a key role in cell growth, survival, and proliferation; hence, their inhibition has been mainly a strategy that targets cancer therapy.[1] PI3Kγ is widely expressed in granulocytes, monocytes, and macrophages, whereas the PI3Kδ isoform is also found in B and T-cells.[1] PI3Kγ and PI3Kδ represent key modulators of innate and adaptive immune responses. PI3Kγ knockout mice showed reduced chemoattractant-induced neutrophil migration to infection sites and respiratory burst.[5−8] Furthermore, PI3Kδ and γ deficiency blocks the

recruitment of neutrophils to inflammation sites.[9,10] PI3Kγ plays a critical role in mediating leukocyte chemotaxis as well as mast cell degranulation, making it a potentially interesting drug target for autoimmune and inflammatory diseases.[11,12] The discovery of PI3Kγ specific inhibitors has faced a daunting challenge due to the high sequence homology at the active site of class I PI3Ks and the conserved topology of the ATP-binding site of the closely related protein kinases such as mTOR and DNA-PK.[13] Compounds with good isoform selectivity are critical tools to study the function of the PI3K pathway and enable the development of treatments that maximize the therapeutic indices.[13b] We previously reported three new classes of potent and isoform selective PI3Kγ inhibitors derived from benzothiazole **1**,[14] thiazolopiperidine **2**,[15] and isoindoline **3**[16] scaffolds as potential therapy for multiple sclerosis (MS) (Figure 1). In an effort to further
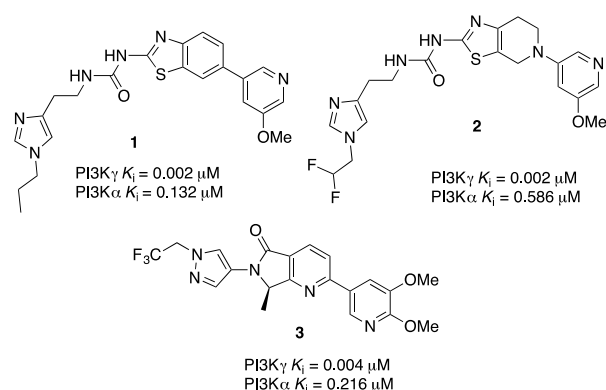
Figure 1. Structures of our previously reported potent and selective PI3Kγ inhibitors.

Figure 3. Chemical structure of the PI3Kγ inhibitor IPI-549.

expand the structural diversity of our potent, selective, and CNS penetrant PI3Kγ inhibitors for the treatment of CNS disorders such as MS, we sought to exploit an alternative scaffold derived from alkynyl thiazole as exemplified by compound **4**. In this paper, we describe the design and synthesis of a highly potent, isoform-selective, and CNS penetrant PI3Kγ inhibitor derived from an alkynylthiazole core (Figure 1).

As we reported previously,[14] benzothiazole urea **1** is a very potent PI3Kγ inhibitor with good isoform selectivity. Our initial design strategy involved the truncation of the benzothiazole to form the alkynyl thiazole core, generating a structurally diverse molecule while maintaining similar potency and selectivity vectors of the benzothiazole core (Figure 2).
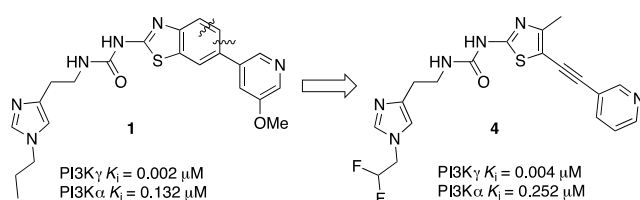

Figure 2. Evolution of the benzothiazole into alkynylthiazole

We discovered that fluoroalkylimidazoles were generally more isoform selective compared to the corresponding alkylimidazoles during the exploration of the thiazolopiperidine series,[15] and thus, we incorporated the difluoromethyl imidazole moiety in the alkynylthiazole series.

The alkyne functionality has been broadly exploited in drug discovery programs, and it brings a number of advantages and disadvantages. The acetylene group has been successfully employed as a nonclassical bioisostere of a wide range of functional groups, including chlorine, iodine, and the nitrile group,[17] but the terminal alkynyl group can also negatively impact drug metabolism through irreversible inhibition of CYP450 enzymes and the formation of GSH conjugates.[17] Alkynyl groups have been previously used in the PI3Kγ inhibitor field. The alkynyl pyrazole-containing **5** (IPI-549) (Figure 3) demonstrated improved potency and high isoform selectivity, with excellent metabolic stability and pharmacokinetic properties.[18]

To optimize the potency and the overall profile of this new series, we performed docking of the proposed new alkynyl thiazole analogs such as compound **4** with PI3Kγ. Using the crystal structure of **1** bound to PI3Kγ (PDB ID 4PS3), we
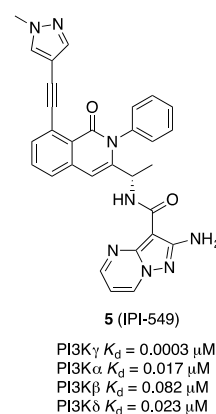
analyzed if it would be possible to maintain or improve the contacts with the protein. The docking results suggested that compound **4** would likely bind in a similar manner to **1**, maintaining a similar conformation and the majority of the contacts. The change in vector space around the methoxypyridine may preclude compound **4** from participation in a water-mediated hydrogen bond network to Tyr867 and Asp841 as seen in several public crystal structures[14] (Figure 4). The loss
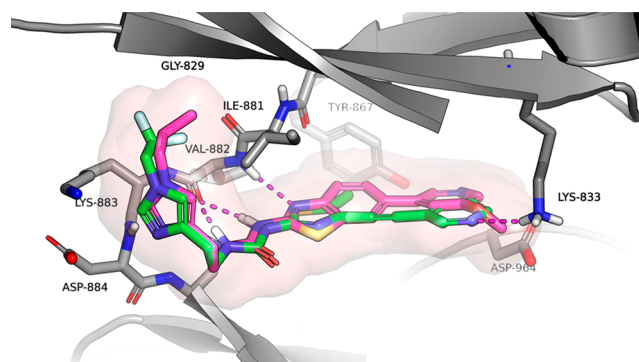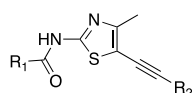

Figure 4. Docking model for compound **4** (green) bound to PI3Kγ and comparison to compound **1** (purple).

of the methoxy group on compound **4** also corresponded to a decrease in docking score and resulted in an inversion of the pyridine nitrogen orientation. The "ring flip" observed in combination with the altered projection of the alkyne from the thiazole core allows for a hydrogen bond between the pyridine nitrogen of **4** and Lys833. Overall, the docking results suggest that the core binding should be maintained and that potency can be gained through a number of interactions.

We first explored the optimization of the urea substituents on the western side of the molecule and the pyridine substitution on the eastern side in the context of the alkynylthiazole core (Table 1). Most of these new analogs exhibit excellent PI3Kγ potency and good selectivity against PI3Kα. Imidazole compounds **4** and **6** showed good selectivity against PI3Kβ (>28-fold). We have previously reported[14] that an introduction of phenoxyethyl urea in the benzothiazole series can increase the PI3Kα selectivity due to unfavorable interaction of the phenyl group with the Asp residue of PI3Kα. However, replacement of the imidazole moiety with an O-aryl group (**7**) failed to improve PI3Kγ potency or PI3Kα selectivity. Replacement of the imidazole moiety with an alkoxy group increased the PI3Kγ potency while maintaining

**Table 1. SAR of Alkynylthiazoles with Varying Pyridine and Urea Substitutions**

Compound	R$_1$	R$_2$	PI3Kγ K_i (nM)	K_i fold α/γ	K_i fold β/γ	K_i fold δ/γ	THP-1^a (MCP-1) IC$_{50}$ (μM)
4	(difluoroethyl imidazole methyl-NH)	pyridine	4	63	50	11	0.13
6	(difluoroethyl imidazole methyl-NH)	pyridine	3	38	28	7	0.1
7	(chlorophenoxyethyl-NH)	pyridine	63	7	-	-	8.2
8	(methoxyethyl-NH)	pyridine	43	2	-		0.76
9	(ethoxyethyl-NH)	pyridine	42	3			0.56
10	(propoxyethyl-NH)	pyridine	6	17	15	18	0.23
11	(dimethylbutoxyethyl-NH)	pyridine	9	48	5	6	0.64
12	(cyclopropylmethoxyethyl-NH)	pyridine	7	28	8	3	0.34

^{a}THP-1 cell assay involves the capacity of the compounds to inhibit PI3Kγ-stimulated phosphorylation of endogenous AKT at Ser-473.
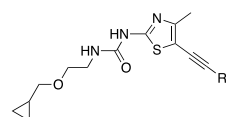
PI3Kα selectivity (10, 11, and 12) whereas compounds with short alkoxyethyl ureas (8, 9) showed poor PI3Kα selectivity. All compounds tested in Table 1 showed a noticeable decrease in cellular potency which is frequently impacted by numerous factors including cell membrane permeability, serum protein binding, off-target activity, and ATP concentration.[19] Imidazole urea compounds (4 and 6) and alkoxy urea compounds (10 and 12) exhibited sub-micromolar cellular potencies. However, compounds 4 and 6 exhibited very poor CNS exposure (B/P ratio < 0.01) as the imidazole is a structural feature that increases the potential for P-gp-mediated efflux (ER 10 and 67 for compounds 4 and 6, respectively). From this list, we selected compound 12 over 11 for further analog generation considering *in vitro* human and rat liver microsomal stability data and cellular potency. Compound 12 displayed better microsomal stability (human and rat) than compound 11 (% remaining after 30 min HLM/RLM 12 92%/85% vs 11 66%/58%), and increased cellular potency (12 = 0.34 μM vs 11 = 0.64 μM). Compound 12 showed low efflux in MDR1-MDCK assay with ER = 1.4.

To better understand the binding mode of the compounds from this new series, an X-ray cocrystal structure of human PI3Kγ in complex with compound 11 (PDB ID 7KKE) was obtained (Figure 5). The 3,3-dimethylbutoxy linker of
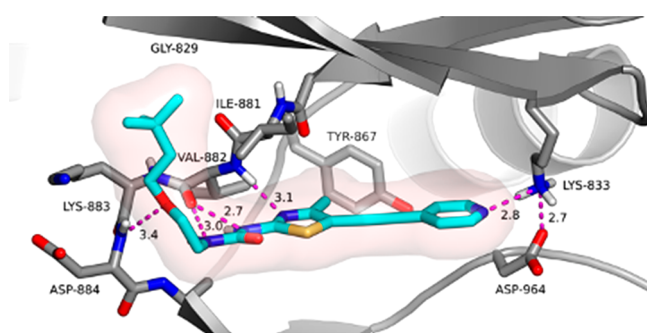
Figure 5. X-ray cocrystal structure of 11 bound to PI3Kγ (PDB ID 7KKE).

compound 11 occupies a hydrophobic pocket adjacent to the ATP-binding site while the linker oxygen makes an H-bond interaction with Asp884. The thiazole nitrogen and the NH of the urea form a bidentate hinge-binding interaction with the backbone carbonyl (C=O) of Val882. As the pyridine atom shifts its location, the pyridine nitrogen no longer participates in the water-mediated H-bond network with Tyr867 and Asp841 as seen in the benzothiazole series.[14] Instead, the pyridine nitrogen makes a favorable H-bond (2.83 Å) interaction with Lys833.

We next explored the SAR of the eastern pyridine group while keeping the *O*-methylcylopropoxyethyl-substituted urea from 12 (Table 2). The methoxy-substituted 3- and 4-
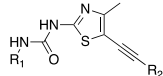
Table 2. SAR of the Pyridine Substitutions

Compound	R$_2$	PI3Kγ K_i (nM)	K_i fold α/γ	K_i fold β/γ	K_i fold δ/γ	THP-1 (MCP-1) IC$_{50}$ (μM)
12	pyridin-4-yl	7	28	8	3	0.34
13	3-OMe-pyridine	11	51	5	0.8	0.51
14	2-OMe-pyridine	3	19	3	3	0.18
15	OMe-pyridine	6	47	4	8	0.41
16	2-OMe-pyridine	240	6	-	-	-
17	2-F-pyridine	6	26	5	11	0.49
18	2-Cl-methylpyridine	10	35	3	3	-
19	CF$_3$-pyridine	52	76	-	-	3.1
20	dimethoxypyrazine	5	31	3	6	0.33
21	quinoline	99	7	3	3	4.3
22	quinoline	6	24	5	3	0.29
23	imidazopyridine	22	52	4	3	0.60
24	azaindole	25	8	3	3	0.49
25	naphthyridine	45	18	4	3	>10
26	pyridopyrazine	11	12	4	5	1.8

pyridines 13, 14, and 15 and 2-fluorine and 2-chlorine substituted 4-pyridines 17 and 18 displayed good PI3Kγ potency and selectivity over the α isoform, but with no improvement in selectivity toward the β or δ subtypes. The methoxy-substituted 2-pyridine (16) did not improve PI3Kγ potency and selectivity over the α isoform. A pyridine analog with a strong electron withdrawing group such as CF$_3$, 19, showed reduced PI3Kγ potency. Dimethoxy substituted pyrazine analog 20 showed good PI3Kγ potency and α

isoform selectivity. Using fused bicycles as replacements for the pyridine in the alkynyl thiazoles led to a consistent reduction in PI3Kγ potency, except for **22** and **26**. Most of these bicyclic-substituted compounds also exhibited reduced PI3Kα selectivity except for compound **23**.

We next introduced chirality to the alkoxy ethyl urea linker aiming to further improve PI3Kγ potency and subtype selectivity (Table 3). Compounds with α-substituted ureas

Table 3. SAR of the Urea Linker Substitutions

Compound	R$_1$	R$_2$	PI3Kγ K_i (nM)	K_i fold α/γ	K_i fold β/γ	K_i fold δ/γ	THP-1 (MCP-1) IC$_{50}$ (μM)
12			7	28	8	3	0.34
27			89	15	-	-	-
28			342	4	-	-	-
29			122	5	5	0.8	3.2
30			9	88	4	6	0.31
31			4	663	6	34	0.38
32			3	53	4	5	0.20
33			4	99	6	9	0.43
34			14	113	-	-	2.7

demonstrated dramatically reduced PI3Kγ potency (**12** vs **27**, **28**). It was observed that the chirality plays a role in the potency gain as the (R)-1-methyl ethoxyurea **27** is 4-fold more potent than the (S)-1-methyl ethoxyurea analogue **28**. Interestingly, β-substituted ethoxyurea maintained good PI3Kγ potency, specifically with the (S)-2-methyl alkoxyurea analogues (**30**, **31**, **32**, and **33**). We envisioned that alkyl substituents in the linker adjacent to the urea might shield its H-bond donor ability and prevent an efficient interaction with Val887 in the hinge region. We observed that several (S)-2-methyl alkoxyurea analogues exhibited excellent PI3Kγ potency and α selectivity (**30**, **31**, **32**, and **33**). Compound **31** showed the best PI3Kα selectivity (663-fold) and PI3Kδ

selectivity (34-fold) while maintaining single-digit nanomolar PI3Kγ potency. The replacement of the cyclopropyl group with a cyclobutyl group slightly decreased PI3Kγ affinity but increased PI3Kα selectivity (**30** vs **34**). However, **34** is 9-fold less potent than **30** in the THP-1 (MCP-1) cellular assay.

We selected a few compounds based on enzymatic potency, cellular potency, and isoform selectivity within the series for further *in vitro* profiling and identification of suitable compounds for pharmacokinetic evaluation (Table 4). However, most of these compounds showed lower potency in our THP-1 cellular assay, which may be due to poor solubility or cell permeability. Our ultimate goal was to identify CNS-penetrant PI3Kγ inhibitors for the potential treatment of CNS disorders such as multiple sclerosis.[16] Therefore, It is very important to maintain low P-gp-mediated efflux, good B/P ratio, and good cell permeability. Our top compounds in Table 4 showed CNS multiparameter optimization (MPO) desirability scores[20] greater than 4. Compounds **14**, **31**, and **32** showed good MDCK-MDR1 cell permeability.[21] We expected reduced CNS exposure for compounds **4** and **23** which are P-gp substrates (ER = 10 and 12, respectively, in rats). The replacement of the difluoromethyl imidazole side chain with a cyclopropylmethoxy group dramatically decreased the efflux ratio (**14**, **31**, and **32**). Compound **32** had the best brain-to-plasma ratio in rats (B/P) as a result of the low MDCK-MDR1 efflux ratio (0.9) and high permeability. The higher lipophilicity (cLogD 3.2) attributed compound **32** accounts for good permeability. Additionally, most of these compounds showed good microsomal stability in human and rats except for compound **31**. One of the key challenges in developing inhibitors of PI3K is cross-inhibition of other protein kinases, most notably mTOR and DNA-PK.[13] All lead compounds in Table 4 exhibited high DNA-PK selectivity profiles, and most of the top compounds did not display hERG liabilities.

Compounds **14**, **23**, and **32** were selected for pharmacokinetic (PK) studies in rats (Table 5). Compounds **14** and **32** exhibited good oral PK profiles with high exposure and excellent bioavailability in rats. However, both of these compounds showed moderate clearance and short half-life in intravenous PK studies. In contrast, compound **23** showed the best intravenous PK profile with the best clearance (12 mL/min/kg) and good half-life (2.6 h) in rats. However, we did not pursue compound **23** further as it was a P-gp substrate (ER = 12).

Based on PK properties in rats, we selected compound **14** to investigate the effect of PI3Kγ inhibition activity in vivo.

Table 4. Overall Profiles for Compounds 4, 14, 23, 31, and 32

	4	14	23	31	32
MW, clogD, PSA	416, 2.7, 85	416, 3.0, 95	395, 2.7, 91	400, 3.0, 85	431, 3.2, 95
THP-1 (MCP-1) IC$_{50}$ (μM)	0.13	0.18	0.60	0.38	0.20
MDCK-MDRI E.R./P_{app}A-B	10/8	2/10	12/4	2/16	0.9/34
Rat B/P[a]	0.013	0.1			0.3
CNS MPO	5.0	4.6	5.1	4.9	4.3
CYP 2C9 IC$_{50}$ (μM)	0.49	7	11	11	15
Microsome stability[b] H/R	92/100	89/69	100/73	56/51	79/100
Protein binding % H/R		98.11/98.88	94.12/92.96	98.66/>99	>99/>99
DNA-PK K_i (μM)	3.4	2.8	>7	>7	3.5
hERG (Planar patch) IC$_{50}$ (μM)	13	>30	>30	28	>30
Kinase selectivity	>4 μM for 13 kinases	>4 μM for 13 kinases	>4 μM for 13 kinases	>4 μM for 13 kinases	>4 μM for 13 kinases

[a]Determined from 1 mg/kg oral dose, 1 h time point. [b]% Remaining after 30 min.

Table 5. IV and PO PK Profiles of Compounds 14, 23, and 32

	14	23	32
Rat IV PK (1mg/kg)			
C1 (mL/min/kg)/Clu	40/3571	12/170	34/3400
$T_{1/2}$ (h)	1	2.6	1
V_{ss} (L/kg)	3	2.3	1.7
Rat PO PK (5mg/kg)			
$AUC_{o\text{-}inf}$ (μg·h/mL)	7.1		6.8
C_{max} (μg/mL)	2.1		1.1
$T_{1/2}$ (h)	1.3		2.7
% F	100		100

Chemoattractant, IL-8 stimulated neutrophil migration into air pouches in mice has previously been shown to be dependent on PI3Kγ.[18] In response to the inflammatory process, PI3Kγ activated immune cells such as neutrophils migrate to the sites of inflammation.[22] To demonstrate PI3Kγ inhibition activity of compound **14** in vivo, we evaluated the effect of orally administered compound **14** (50 mg/kg) on IL-8 stimulated neutrophil migration into the air pouches on mice. Compound **14** significantly reduced (85%) neutrophil recruitment into the air pouches at a 50 mg/kg dose and exhibited good brain exposure with a B/P of 0.43 at 4 h postdosing (Figure 6). This result demonstrates that orally administered compound **14** can inhibit PI3Kγ activation *in vivo*.
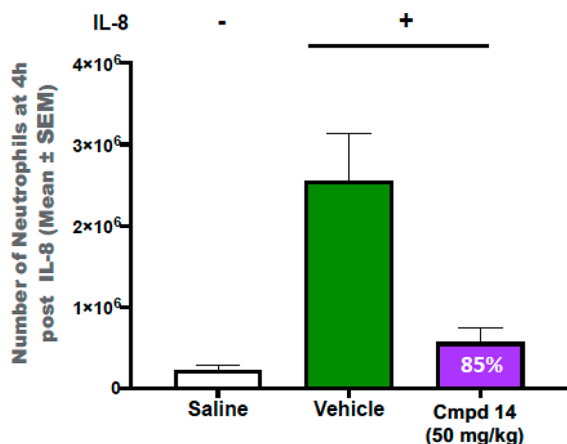

Figure 6. Effect of compound **14** on neutrophil migration in the mouse air pouch model.

The general syntheses of alkynylthiazoles, exemplified by compounds **4, 13**, and **17**, are shown in Schemes 1 and 2. In Scheme 1, the five-step sequence starts with the commercially available thiazole amide **35**. The iodination of **35** with NIS followed by Sonagashira coupling with 3-ethynylpyridine afforded compound **37** in good yield. The removal of the acetyl group of **37** with hydrazine hydrate afforded compound **38** in 77% yield. Activation of compound **38** with CDI followed by coupling with 2-(1-(2,2-difluoroethyl)-1H-imidazol-4-yl)ethan-1-amine afforded target compound **4** in moderate yield.

Compounds **13** and **17** were synthesized as shown in Scheme 2 (routes 1 and 2). Activation of compound **40** with CDI followed by coupling with 2-(cyclopropylmethoxy)-ethanamine afforded compound **41** in 45% yield. Sonagashira coupling with **41** with 3-methoxy-5-((trimethylsilyl)ethynyl)-

Scheme 1. Synthesis of Alkynylthiazole 4[a]
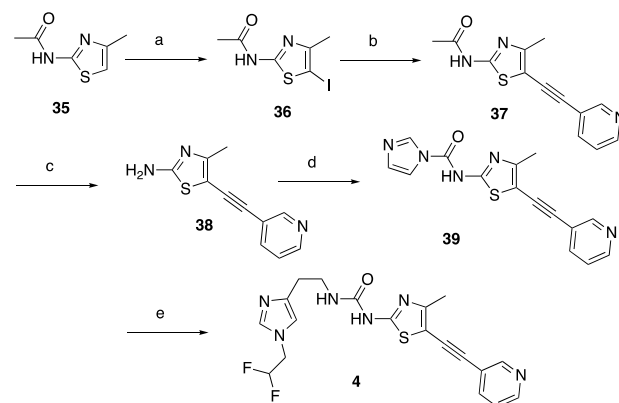
[a]Reagents and conditions: (a) NIS, DCM, r.t, 10 min, 66%; (b) 3-ethynylpyridine, Pd(PPh$_3$)$_4$, CuI, Et$_3$N, dioxane, r.t., 1.5 h, 77%; (c) hydrazine hydrate, THF, 85 °C, 6 h, 77%; (d) CDI, DMF, 70 °C, 2 h, 92%; (e) 2-(1-(2,2-difluoroethyl)-1H-imidazol-4-yl)ethan-1-amine, Et$_3$N, THF, r.t., 20 h, 58%.

Scheme 2. Synthesis of Alkynylthiazoles 13 and 17[a]
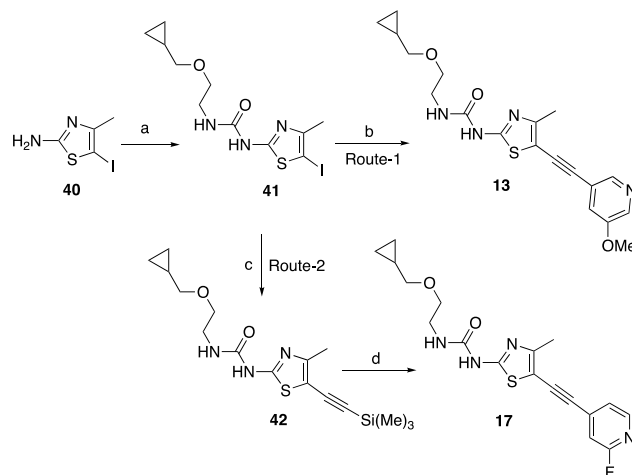
[a]Reagents and conditions: (a) CDI, DCM, 2-(cyclopropylmethoxy)-ethanamine, 60 °C, 2 h, 45%; (b) 3-methoxy-5-((trimethylsilyl)-ethynyl)pyridine, PdCl$_2$(PPh$_3$)$_2$, CuI, TEA, TBAF, THF, 64 °C, 1 h, 41%; (c) ethynyl(trimethyl)silane, CuI, Pd(PPh$_3$)$_2$, TEA, THF, 65 °C, 1 h, 58%; (d) 2-fluoro-3-iodopyridine, CuI, Pd(PPh$_3$)$_2$, TEA, TBAF, THF, 65 °C,1 h.

pyridine in the presence of TBAF afforded compound **13** in 41% yield. The Sonagashira coupling of **41** with ethynyl-(trimethyl)silane compound **42** gave 58% yield. The second Sonagashira coupling of **42** with 2-fluoro-3-iodopyridine in the presence of TBAF afforded compound **17** in 50% yield.

In summary, we have designed and synthesized a new series of highly potent and isoform selective inhibitors of PI3Kγ using structure-guided drug design based on our earlier reported work in this area. The SAR study focused on optimizing the *in vitro* potency, the isoform selectivity, and the ADME profile of the compounds in order to find lead compounds. The lead compounds **14** and **32** showed good *in vitro* metabolic stability in rat and human liver microsomes and good *in vivo* pharmacokinetic properties in rat, along with good CNS exposure. Compound **14** showed *in vivo* efficacy in a mouse air pouch model by reducing neutrophil migration in 85% at 50

mg/kg dose. The potent PI3Kγ inhibitors identified within this series can thus serve as suitable *in vivo* tool compounds.

AUTHOR INFORMATION

Corresponding Author

Upul K. Bandarage − *Vertex Pharmaceuticals Incorporated, Boston, Massachusetts 02210, United States;* orcid.org/0000-0002-9456-6181; Phone: 617-341-6882; Email: upul_bandarage@vrtx.com

Authors

Alex M. Aronov − *Vertex Pharmaceuticals Incorporated, Boston, Massachusetts 02210, United States*

Jingrong Cao − *Vertex Pharmaceuticals Incorporated, Boston, Massachusetts 02210, United States*

Jon H. Come − *Vertex Pharmaceuticals Incorporated, Boston, Massachusetts 02210, United States*

Kevin M. Cottrell − *Vertex Pharmaceuticals Incorporated, Boston, Massachusetts 02210, United States*

Robert J. Davies − *Vertex Pharmaceuticals Incorporated, Boston, Massachusetts 02210, United States*

Simon Giroux − *Vertex Pharmaceuticals Incorporated, Boston, Massachusetts 02210, United States;* orcid.org/0000-0003-1499-2576

Marc Jacobs − *Vertex Pharmaceuticals Incorporated, Boston, Massachusetts 02210, United States*

Sudipta Mahajan − *Vertex Pharmaceuticals Incorporated, Boston, Massachusetts 02210, United States*

David Messersmith − *Vertex Pharmaceuticals Incorporated, Boston, Massachusetts 02210, United States*

Cameron S. Moody − *Vertex Pharmaceuticals Incorporated, Boston, Massachusetts 02210, United States*

Rebecca Swett − *Vertex Pharmaceuticals Incorporated, Boston, Massachusetts 02210, United States*

Jinwang Xu − *Vertex Pharmaceuticals Incorporated, Boston, Massachusetts 02210, United States*

Complete contact information is available at:
https://pubs.acs.org/10.1021/acsmedchemlett.0c00573

Notes

The authors declare no competing financial interest.
All authors are current or former employees of Vertex Pharmaceuticals Incorporated.

ABBREVIATIONS

CNS, central nervous system; MCP-1, monocyte chemoattractant protein 1; MDCK, Madin Darby; MDR1, multidrug resistance mutation 1; GPCR, G-protein-coupled receptor; PgP, P-glycoprotein-1; ER, efflux ratio; NIS, N-iodosuccinimide; CDI, N,N′-carbonyldiimidazole; DCM, dichloromethane; TBAF, tetra-n-butylammonium fluoride; THF, tetrahydrofuran

REFERENCES

(1) Banham-Hall, E.; Clatworthy, M. R.; Okkenhaug, K. The Therapeutic Potential for PI3K Inhibitors in Autoimmune Rheumatic Diseases. *Open Rheumatol. J.* **2012**, *6*, 245−258.

(2) Cantley, L. C. The phosphoinositide 3-kinase pathway. *Science* **2002**, *296* (5573), 1655−1657.

(3) Vanhaesebroeck, B.; Guillermet-Guibert, J.; Graupera, M.; Bilanges, B. The emerging mechanisms of isoform-specific PI3K signaling. *Nat. Rev. Mol. Cell Biol.* **2010**, *11*, 329−341.

(4) Vanhaesebroeck, B.; Leevers, S. J.; Ahmadi, K.; Timms, J.; Katso, R.; Driscoll, P. C.; Woscholski, R.; Parker, P. J.; Waterfield, M. D. Synthesis and function of 3-phosphorylated inositol lipids. *Annu. Rev. Biochem.* **2001**, *70*, 535−602.

(5) Sasaki, T.; Irie-Sasaki, J.; Jones, R. G.; Oliveira-Dos-Santos, A. J.; Stanford, W. L.; Bolon, B.; Wakeham, A.; Itie, A.; Bouchard, D.; Kozieradzki, I.; Joza, N.; Mak, T. W.; Ohashi, P. S.; Suzuki, A.; Penninger, J. M. Function of PI3Kgamma in thymocyte development, T cell activation, and neutrophil migration. *Science* **2000**, *287*, 1040−1046.

(6) Hirsch, E.; Katanaev, V. L.; Garlanda, C.; Azzolino, O.; Pirola, L.; Silengo, L.; Sozzani, S.; Mantovani, A.; Altruda, F.; Wymann, M. P. Central role for G protein-coupled phosphoinositide 3-kinase gamma in inflammation. *Science* **2000**, *287*, 1049−1053.

(7) Li, Z.; Jiang, H.; Xie, W.; Zhang, Z.; Smrcka, A. V.; Wu, D. Roles of PLC-beta2 and-beta3 and PI3Kgamma in chemoattractant mediated signal transduction. *Science* **2000**, *287*, 1046−1049.

(8) Condliffe, A. M.; Davidson, K.; Anderson, K. E.; Ellson, C. D.; Crabbe, T.; Okkenhaug, K.; Vanhaesebroeck, B.; Turner, M.; Webb, L.; Wymann, M. P.; Hirsch, E.; Ruckle, T.; Camps, M.; Rommel, C.; Jackson, S. P.; Chilvers, E. R.; Stephens, L. R.; Hawkins, P. T. Sequential activation of class IB and class IA PI3K is important for the primed respiratory burst of human but not murine neutrophils. *Blood* **2005**, *106*, 1432−1440.

(9) Hirsch, E.; Katanaev, V. L.; Garlanda, C.; Azzolino, O.; Pirola, L.; Silengo, L.; Sozzani, S.; Mantovani, A.; Altruda, F.; Wymann, M. P. Central role for G protein-coupled phosphoinositide 3-kinase gamma in inflammation. *Science* **2000**, *287*, 1049−53.

(10) Puri, K. D.; Doggett, T. A.; Douangpanya, J.; Hou, Y.; Tino, W. T.; Wilson, T.; Graf, T.; Clayton, E.; Turner, M.; Hayflick, J. S.; Diacovo, T. G. Mechanisms and implications of phosphoinositide 3-kinase delta in promoting neutrophil trafficking into inflamed tissue. *Blood* **2004**, *103*, 3448−56.

(11) Camps, M.; Rückle, T.; Ji, H.; Ardissone, V.; Rintelen, F.; Shaw, J.; Ferrandi, C.; Chabert, C.; Gillieron, C.; Francon, B.; Martin, T.; Gretener, D.; Perrin, D.; Leroy, D.; Vitte, P. A.; Hirsch, E.; Wymann, M. P.; Cirillo, R.; Schwarz, M. K.; Rommel, C. Blockade of PI3K., suppresses joint inflammation and damage in mouse models of rheumatoid arthritis. *Nat. Med. (N. Y., NY, U. S.)* **2005**, *11*, 936−943.

(12) Wymann, M. P.; Bjoerkloef, K.; Calvez, R.; Finan, P.; Thomast, M.; Trifilieff, A.; Barbier, M.; Altruda, F.; Hirsch, E.; Laffargue, M. Phosphoinositide 3-kinase.,: a key modulator in inflammation and allergy. *Biochem. Soc. Trans.* **2003**, *31*, 275−280.

(13) Sundstrom, T. J.; Anderson, A. C.; Wright, D. L. Inhibitors of phosphoinositide-3-kinase: a structure-based approach to understanding potency and selectivity. *Org. Biomol. Chem.* **2009**, *7*, 840−850.

(14) Collier, P. N.; Martinez-Botella, G.; Cornebise, M.; Cottrell, K. M.; Doran, J. D.; Griffith, J. P.; Mahajan, S.; Maltais, F.; Moody, C. S.; Huck, E. P.; Wang, T.; Aronov, A. M. Structural basis for isoform selectivity in a class of benzothiazole inhibitors of phosphoinositide 3-kinase γ. *J. Med. Chem.* **2015**, *58*, 517−521.

(15) Collier, P. N.; Messersmith, D.; Le Tiran, A.; Bandarage, U. K.; Boucher, C.; Come, J.; Cottrell, K. M.; Damagnez, V.; Doran, J. D.; Griffith, J. P.; Khare-Pandit, S.; Krueger, E. B.; Ledeboer, M. W.;

Ledford, B.; Liao, Y.; Mahajan, S.; Moody, C. S.; Roday, S.; Wang, T.; Xu, J.; Aronov, A. M. Discovery of highly isoform selective thiazolopiperidine inhibitors of of phosphoinositide 3-kinaseb. *J. Med. Chem.* **2015**, *58*, 5684−5688.

(16) Come, J. H.; Collier, P. N.; Henderson, J. A.; Pierce, A. C.; Davies, R. J.; Le Tiran, A.; O'Dowd, H.; Bandarage, U. K.; Cao, J.; Deininger, D.; Grey, R.; Krueger, E. B.; Lowe, D. B.; Liang, J.; Liao, Y.; Messersmith, D.; Nanthakumar, S.; Sizensky, E.; Wang, J.; Xu, J.; Chin, E. Y.; Damagnez, V.; Doran, J. D.; Dworakowski, W.; Griffith, J. P.; Jacobs, M. D.; Khare-Pandit, S.; Mahajan, S.; Moody, C. S.; Aronov, A. M. Design and Synthesis of a Novel Series of Orally Bioavailable, CNS-Penetrant, Isoform Selective Phosphoinositide 3-KinaseK (PI3K) Inhibitors with Potential for the Treatment of Multiple Sclerosis (MS). *J. Med. Chem.* **2018**, *61*, 5245−5256.

(17) Talele, T. T. Acetylene Group, Friend or Foe in Medicinal Chemistry. *J. Med. Chem.* **2020**, *63*, 5625−5663.

(18) Liu, T.; Lescarbeau, A.; Nair, S. J.; Grenier, L.; Pradeilles, J. A.; Glenadel, Q.; Tibbitts, T.; Rowley, A. M.; DiNitto, J. P.; Brophy, E. E.; O'Hearn, E. L.; Ali, J.; Evans, C. AA.; Winkler, D. G.; Goldstein, S. I.; O'Hearn, P.; Martin, C. M.; Hoyt, J. G.; Soglia, J. R.; Cheung, C.; Pink, M. M.; Proctor, J. L.; Palombella, V. J.; Tremblay, M. R.; Castro, A. C. Discovery of a selective phosphoinositide-3-kinase (PI3K)-gamma inhibitor (IPI-549) as an immuno-oncology clinical candidate. *ACS Med. Chem. Lett.* **2016**, *7*, 862−867.

(19) Schwaid, A. G.; Cornella-Taracido, I. Causes and Significance of Increased Compound Potency in Cellular or Physiological Contexts. *J. Med. Chem.* **2018**, *61*, 1767−1773.

(20) Wager, T. T.; Hou, X.; Verhoest, P. R.; Villalobos, A. Moving beyond rules: the development of a central nervous system multiparameter optimization (CNS MPO) approach to enable alignment of druglike properties. *ACS Chem. Neurosci.* **2010**, *1*, 435−449.

(21) Volpe, D. A.; et al. Drug-permeability and transporter assays in Caco-2 and MDCK cell lines. *Future Med. Chem.* **2011**, *3*, 2063−2077.

(22) Sasaki, T.; Irie-Sasaki, U.; Jones, R. G.; Oliveira-Do-Santos, A. J.; Stanford, W. L.; Bolon, B.; Wakeham, A.; Itie, A.; Bouchard, D.; Kozieradzki, I.; Joza, N.; Mak, T. W.; Ohashi, P. S.; Suzuki, A.; Penninger, J. M. Function of PI3K in thymocyte development, T cell activation, and neutrophil migration. *Science* **2000**, *287*, 1040−1046.